Cold Neutron Prompt Gamma Activation Analysis, a Non-destructive Technique for Hydrogen Level Assessment in Zirconium Alloys

Adrien Couet[a], Arthur T. Motta[a*],

[a]Department of Mechanical and Nuclear Engineering, Penn State University, University Park, PA, USA, 16802

Robert J. Comstock[b],

[b]Research and Technology Unit, Westinghouse Electric Company, Pittsburgh, PA, USA, 15235

and

Rick L. Paul[c]

[c]National Institute of Standards and Technology, Gaithersburg, MD, USA, 20899

* Corresponding author:
    Tel: 814-865-0036
    Email: atm2@psu.edu

1

Abstract

We propose a novel use of a non-destructive technique to quantitatively assess hydrogen concentration in zirconium alloys. The technique, called Cold Neutron Prompt Gamma Activation Analysis (CNPGAA), is based on measuring prompt gamma rays following the absorption of cold neutrons, and comparing the rate of detection of characteristic hydrogen gamma rays to that of gamma rays from matrix atoms. Because the emission is prompt, this method has to be performed in a reactor such at the National Institute of Technology (NIST). Determination is simple and is shown here to be accurate, matching the results given by usual destructive techniques such as Vacuum Hot Extraction (VHE), with a precision of ± 2mg.kg^{-1} (or wt.ppm). Very low levels of hydrogen (as low as 5wt.ppm) can be detected. Also, it is demonstrated that CNPGAA can be used sequentially on an individual corrosion coupon during autoclave testing, to measure a gradually increasing hydrogen concentration. Thus, this technique can replace destructive techniques performed on "sister" samples, which inherently yield greater experimental uncertainty results. In this study, the technique is developed for use in the measurement of hydrogen concentration in zirconium alloys.

1. Introduction

With increased burnups and longer life times in nuclear reactors, uniform corrosion of zirconium alloy nuclear fuel cladding and the associated hydrogen pick-up can become a life-limiting degradation mechanism in existing and advanced light water reactors, since the ingress of hydrogen and precipitation of hydrides can cause cladding embrittlement [1, 2]. Thus, it is of great interest to limit cladding embrittlement by decreasing overall corrosion and/or by decreasing the amount of hydrogen ingress for a given corrosion rate. The corrosion reaction is given by:

$$Zr + 2H_2O \rightarrow ZrO_2 + 2H_2 \qquad (1)$$
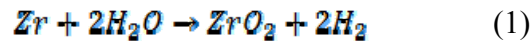
Some of the hydrogen generated during corrosion can enter the metal. The hydrogen picked up by the metal during reactor or autoclave exposure is normalized to the hydrogen generated in the corrosion reaction. We define the hydrogen pick-up fraction f_H as the ratio of the hydrogen absorbed by the metal over the overall generated hydrogen:

$$f_H = \frac{H_{absorbed}}{H_{generated}} \qquad (2)$$

Despite extensive research, the mechanisms of hydrogen pick-up and especially the influence of the alloy composition and microstructure on f_H are not at all well understood [3-6]. In addition, there is evidence that f_H may vary during the corrosion process, such that different values occur at different stages of oxide film growth [7]. Part of the difficulty in developing mechanistic understanding of hydrogen pick-up is that reliable and precise measurements of hydrogen pick-up during corrosion are difficult to obtain. The purpose of this study is to demonstrate the use of Cold Neutron Prompt Gamma Activation Analysis (CNPGAA) to investigate the variations of f_H with alloy composition, corrosion time and alloy microstructure. In order to achieve this purpose,

differences as low as 5mg.kg^{-1} need to be precisely measured in zirconium alloys. Note because the hydrogen masses, alloying element content and weight gain due to corrosion are very low, mg.kg^{-1} is for all practical purposes equal to wt. ppm; this last unit will be used as this is the common unit of hydrogen in zirconium.

Many techniques have been traditionally used to measure hydrogen content in zirconium. Destructive techniques such as Vacuum Hot Extraction (VHE) or Inert Gas Fusion (IGF) have been widely used in past research [3-5, 8]. These techniques are well developed, fast and inexpensive. In these experiments, zirconium samples are heated either to 1200 °C in the case of VHE (causing significant alloy microstructure changes, since the zirconium transition from α to β phase occurs at 865 °C) or to above the melting temperature in the case of IGF. Thus, both VHE and IGF are destructive techniques, which preclude further analyses on the sample. Hence, sister samples (identical samples coming from the same batch of material) must to be used to evaluate the hydrogen pick-up variation as a function of corrosion time, which inherently spreads the results and makes the induced error difficult to evaluate. Also, the sample size analyzed in VHE and IGF (a piece of approximately 4mm x 8mm) is much smaller than a standard corrosion coupon (25mm x 20mm). Thus, spot-to-spot hydrogen concentration variations within the coupon may falsify the results. Finally the precision of these destructive techniques at these low hydrogen concentration levels is not well established.

Various non-destructive techniques have been used for evaluating hydrogen content in zirconium alloys. The EMAR method (electromagnetic acoustic resonance) [9] is ideal for in situ measurement but is not very precise. Also ultrasonic measurement coupled with eddy current testing [10], or neutron transmission technique [11] have been applied to this problem . However

none of these techniques have the level of reliability and precision required to detect low hydrogen concentration levels in zirconium alloys.

In this study we use CNPGAA to analyze low levels of hydrogen in zirconium. CNPGAA has not been routinely used to detect hydrogen in zirconium alloys, as it is time consuming and can only be performed in a specialized facility. As will be shown, this technique is non-destructive, precise, measures the average hydrogen concentration in the whole sample and can detect very low levels of hydrogen (as low as 5 wt.ppm).

The initial results from CNPGAA are presented in this paper.

2. Experimental procedures

2.1. VHE and IGF apparatus

Vacuum Hot Extraction and Inert Gas Fusion have been performed by LUVAK, Inc. at Boylston. A NRC Model 917* apparatus [12] has been used for VHE. A weighed sample is introduced through a vacuum lock into a molybdenum crucible in a vacuum line system. Prior to analysis, the sample is cleaned with ether and allowed to dry to remove any surface contamination. Heat is then applied to the crucible through an induction coil, to heat the sample and crucible to just below the melting point of the sample and with the aid of high speed diffusion pumps, the hydrogen released is extracted from the sample and collected within the system. The amount of hydrogen present is then measured using a McLeod gauge and results are reported in parts per million by weight.

A Leco RH-404 Hydrogen Analyzer* apparatus [13] has been used for IGF. A weighed sample is melted in a graphite crucible in a stream of high purity argon. Molecular hydrogen is released from the sample and is separated from any carbon monoxide and nitrogen liberated from the

sample. A thermal conductivity cell determines the hydrogen content from which the weight percent of hydrogen in the sample is calculated. The calibration of the VHE and IGF hydrogen determinations is verified with a NIST traceable standard reference material of hydrogen into titanium [14].

2.2. CNPGAA apparatus

CNPGAA was performed at National Institute of Standards and Technology (NIST), Gaithersburg, in one of the cold neutron beam lines. A scheme of the whole apparatus is presented in Figure 1 and precise details on the apparatus are described elsewhere [15-17]. A brief description of the technique is presented here. The CNPGAA detection technique is based on the emission of characteristic prompt gamma rays emitted by a given nucleus when it absorbs a neutron. Thermal neutrons exit the nuclear reactor ($E_{neutrons} \cong 0.025 eV$) and enter a liquid hydrogen cold moderator ($T_{moderator} \approx 25K$), which shifts the neutron spectrum to lower energy ($E_{neutrons} \cong 5 meV$). In a slightly curved neutron guide over a distance of 41m, gamma rays and fast neutrons travel straight out the guide while cold neutrons are efficiently reflected and guided to the sample, thus providing a nearly pure beam of cold neutrons on the sample. These neutrons pass a collimator and are incident on the sample on a circular area of approximately 3.14cm^2. The neutrons go through the sample, so the hydrogen content is averaged through the sample thickness. Some neutrons are absorbed by the sample, some by the chamber, and some pass through the chamber without being absorbed (the probability of

absorption depends on the cross sections). Cold neutrons are necessary since the absorption rate increases significantly when the neutron velocity decreases. Indeed, the hydrogen capture cross section is inversely proportional to the velocity at thermal neutron energies, such that neutrons from a moderator at 30 K yield an approximately threefold higher hydrogen reaction rate than those from a 300 K source. Absorption of cold neutrons by hydrogen results in the emission within 10^{-9} seconds of one characteristic gamma ray at the energy of 2223keV, due to the single hydrogen nucleus de-excitation ($^1H(n,\gamma)\,^2H$). This gamma ray is then detected and the signal can be converted to the hydrogen concentration of the sample. The neutron flux at the CNPGGA target position is approximately $8 \times 10^8\ neutrons.\,cm^{-2}.\,s^{-1}$.

The inner chamber (24.1 cm x 17.1 cm x 24.8 cm) is made of aluminum and magnesium alloys which have small neutron absorption cross section. This minimizes the gamma ray background from neutron capture by the walls of the sample box. The chamber is purged with helium to minimize the gamma ray background due to neutron capture by nitrogen and hydrogen in atmospheric water vapor. Samples irradiated inside the chamber are suspended by Teflon strings between the prongs of an aluminum fork (again to minimize the instrumental background). The samples are thin enough to avoid gamma ray attenuation and self-shielding inside the sample and we can assume that the neutron absorption is homogeneous within the sample.

Gamma rays emitted by the sample are measured using a high purity germanium detector mounted vertically into a bismuth germanate (BGO) Compton suppressor (which improves the signal-to-noise ratio by decreasing the baseline background coming from Compton gamma-rays). Accounting for all of these features, the maximum background noise at the hydrogen gamma ray energy is 5 wt.ppm, such that very low concentrations of hydrogen in the samples are detectable.

This background is principally coming from other gamma-rays produced by neutron capture in hydrogenous materials present in germanium and BGO detectors.

2.3. Fitting programs

During the experiment a gamma ray spectrum is acquired in which each peak is originated from a given gamma ray of a given nucleus de-excitation. Although the hydrogen nucleus undergoes only one characteristic nuclear de-excitation (at 2223 keV), zirconium undergoes multiple de-excitations which generate numerous peaks in the gamma-ray spectrum. A typical example of the full gamma ray spectrum of a hydrided zirconium alloy is shown in Figure 2, with a zoom on the hydrogen peak energy region given in Figure 3. The zirconium 934 keV peak has been chosen as the reference zirconium peak. Different types of fitting programs have been used to analyze the results. Indeed, since the detected hydrogen concentrations can be very low, the choice of the fitting programs can affect the results. To verify this, three different fitting programs were used: an algorithm for hand fitting of peaks (SUM) written at NIST [18], a standard commercial peak search program which locates peaks and integrates peaks automatically, and the program PEAKFIT 4.0*, a manual program in which the fitting is made peak by peak and is used to double check the automatic fitting processes used in the other programs. One significant

difference between the SUM algorithm and the standard peak search is that using SUM, the background and peak regions are chosen by hand, while the peak search program chooses a few channels on either side of the peak for background calculation. This different way to consider the background affects the results of the standard peak search, which are always a few wt.ppm lower than the results obtained by SUM.

2.4. Materials examined

2.4.1. Standards

The first major obstacle to performing quantitative hydrogen analysis is that no certified NIST standards of hydrogen in zirconium exist since only destructive techniques are available to precisely detect low hydrogen concentration levels.

The peaks have different sensitivities to the neutron absorption. Sensitivities (the number of counts per seconds per milligrams of the considered element exposed to the beam) are directly related to the neutron absorption cross sections and to the probability of a given de-excitation path compared to another one (for instance going from energy level 1 to 3 directly or passing by the energy level 2). The hydrogen mass fraction in mg.kg^{-1} in a zirconium sample is given by eq.3:

$$C_H^{Sample} = \left(\frac{\frac{A_{2223}}{t} - H_{bkgd}}{S_{2223}^H} \right) \times \left(\frac{S_{934}^{Zr}}{\frac{A_{934}}{t}} \right) \times \frac{10^{-6}}{\omega_{Zr}}\ mg.kg^{-1} \qquad (3)$$

where C_H^{Sample} is the hydrogen concentration in the sample in wt.ppm, A_{2223} is the area of the 2223keV peak in counts, H_{bkgd} is the hydrogen background in counts per second, S_{2223}^H is the hydrogen sensitivity in $cps.mg^{-1}$, t is the acquisition time in seconds, S_{934}^{Zr} is the 934 keV reference zirconium peak sensitivity, A_{934} is the area of the 934 keV reference peak and ω_{Zr} is the mass fraction of zirconium. Considering the extreme low amount of alloying elements in a sample, and the low effect of the oxide formation on the total mass of the sample, we will consider that $\omega_{Zr} \cong 1$ for all alloys and at any time of the corrosion process (and thus mg.kg^{-1} is approximately equal to wt.ppm).

Thus the determination of the sensitivities is of primary importance to the determination of hydrogen concentration. These sensitivities are determined using standards.

Because NIST certified standards of hydrogen into zirconium do not exist (only reference values exist), a combination of different standards had to be used: a pure Zirconium foil ($m_{Zr} = 218mg$), a Titanium foil ($m_{Ti} = 14\ mg$) and a graphite/urea/titanium powder sample (%Ti =12.55% and %H =3.171%). Using this combination of standards, the sensitivities have been calculated using equations 4 to 8:

$$S_{1381}^{Ti} = \frac{A_{1381}}{(m_{Ti} \times t)} \qquad (4)$$

where S_{1381}^{Ti} is the sensitivity of the 1381keV titanium peak, A_{1381} is the area of the 934keV peak and t the acquisition time.

$$S_{934}^{Zr} = \frac{A_{934}}{(m_{Zr} \times t)} \qquad (5)$$

where S_{934}^{Zr} is the sensitivity of the 934keV zirconium peak.

The hydrogen background H_{bkgd} is determined before running the samples by acquiring a spectrum with no sample inserted in the chamber for 48 hours:

$$H_{bkgd} = \frac{A_{2223}}{t} \qquad (6)$$

The ratio of Ti and H sensitivities is determined using the graphite/urea/titanium powder according to:

$$\left(\frac{S_{2223}^{H}}{S_{1381}^{Ti}}\right)_{powder} = \left(\frac{\left(\frac{A_{2223}}{t} - H_{bkgd}\right)}{\%H}\right) \times \left(\frac{\%Ti}{(A_{1381} \times t)}\right) \qquad (7)$$

Finally:

$$S_{2223}^{H} = \left(\frac{S_{2223}^{H}}{S_{1381}^{Ti}}\right)_{powder} \times S_{1381}^{Ti} \qquad (8)$$

The results obtained using the various fitting programs for the analysis and calculation of area are in good agreement with each other. The peak search program gives us the smallest error range and consequently the best confidence. Thus, we will only display the results given by this peak search program. The sensitivities are given in Table 1.

Parameter	Peak centroid (keV)	Peak search program
Zirconium sensitivity (counts.s^{-1}.mg^{-1})	934	9.91×10^{-2} $\pm 7.8 \times 10^{-4}$
Hydrogen sensitivity (counts.s^{-1}.mg^{-1})	2223	13.12 $\pm 2.9 \times 10^{-1}$
Hydrogen background (counts.s^{-1})	2223	6.3×10^{-2} $\pm 1.1 \times 10^{-3}$

Table 1: Hydrogen and Zirconium sensitivities and hydrogen background determined for CNPGAA measurements

2.4.2. Zirconium alloys samples

Corrosion tests were performed at Westinghouse Laboratory in Monroeville. The zirconium alloys samples studied are in the form of corrosion coupons (25 mm x 20 mm x 0.8 mm) and their composition is listed in Table 2 (where the alloying content is indicated in weight percent). The processing of these alloys is described elsewhere [19]. The coupons of various zirconium alloys (including ZrFeCr model alloys, ZrNb and Zircaloy4) were corroded in 360 °C pure water in a single static 4 liter autoclave in saturated pressure condition at 2708.6 psi (18.7 MPa) according to ASTM G2-88 [12]. The alloys underwent different corrosion exposure times and thus exhibit various oxide thicknesses and hydrogen concentrations.

3. Results

3.1. Comparison with destructive techniques

One of the advantages of the CNPGAA technique is that it does not require any information such as precise thickness of the sample or sample weight since the ratios are measured. Using the element ratio method also largely negates the effect of uncertainties concerning neutron interactions (absorption, scattering,…) on the results. Indeed, sources of uncertainties associated with the neutron flux such as beam attenuation, temporal differences in the neutron flux, variation in sample area coverage by the beam or attenuation of the beam into the sample due to neutron absorption will vary from experiment to experiment. However, in a single experiment, these uncertainties are canceled by the element ratio method since they affect both the hydrogen and the zirconium peaks [20]. If we recall eq.1 including uncertainties associated with one particular experiment (denoted by the factor I):

$$C_H^{Sample}(I) = \left(\frac{\frac{I \times A_{2223}}{t} - \frac{I}{t} \times H_{bkgd}}{S_{2223}^H} \right) \times \left(\frac{S_{934}^{Zr}}{\frac{I \times A_{934}}{t}} \right) = C_H^{Sample} \qquad (9)$$

The uncertainty in VHE is the total experimental uncertainty taking into account the technical error coming from the VHE technique and other uncertainties such as the area-to-area variation of hydrogen concentrations in a coupon. This error is difficult to evaluate but using the technical error given by the company [21] and using VHE on various spots of the same coupon, the overall error has been estimated to be equal to ± 1 wt.ppm for every 25 wt.ppm. The error in CNPGAA comes from the error in A_x given by the different fitting programs and the composition errors of the standards. Using propagation error formulas the final error is given by:

$$\Delta C_H^{sample} = C_H^{sample} \times \left(\left(\left(\frac{\sqrt{\left(\left(\frac{\Delta A_{2223}}{t} \right)^2 + \Delta H_{bkgd}^2 \right)}}{\frac{A_{2223}}{t} - H_{bkgd}} \right)^2 + \left(\frac{\Delta S_{2223}^H}{S_{2223}^H} \right)^2 \right)^2 + \left(\left(\frac{\Delta S_{934}^{Zr}}{S_{934}^{Zr}} \right)^2 + \left(\frac{\Delta A_{934}}{A_{934}} \right)^2 \right)^2 \right)^{\frac{1}{2}} \qquad (10)$$

where ΔX denotes the error associated to X.

For benchmarking, ten uncut corrosion coupons were examined using first Cold Neutron Prompt Gamma Activation Analysis and then Vacuum Hot Extraction. The results of this comparison between the two techniques are shown in Table 2.

We notice a consistent difference of approximately 29 wt.ppm (29.4 ± 1.1 wt.ppm with a standard deviation of 1.1wt.ppm) is obtained between the VHE and CNPGAA results. This difference is rationalized and explained in the following part.

Alloys	Exposure time (days)	Hydrogen concentration (wt.ppm) by VHE	Hydrogen concentration (wt.ppm) by CNPGAA
Zr-0.2Fe-0.1Cr	0	11 ± 1	39.8 ± 0.6
	7	24 ± 1	52.9 ± 1.0
	173	64 ± 3	92.0 ± 1.3
Zr-0.4Fe-0.2Cr	493	129 ± 6	160.0 ± 2.1
Zircaloy-4: Zr-0.2Fe-0.1Cr - 1.3Sn	0	9 ± 1	37.3 ± 0.6
	28	23 ± 1	50.0 ± 0.8
	55	25 ± 2	55.4 ± 0.9
	240	75 ± 4	108.0 ± 1.7
Zr-0.2Nb	326	69 ± 3	96.9 ± 1.6
Zr-2.5Nb	326	134 ± 6	165.0 ± 2.2

Table 2: Hydrogen concentration in wt.ppm obtained with VHE and CNPGAA on 10 Zr alloys (25 mm x 20 mm x 0.8 mm) Uncertainties are 1s, based on counting statistics, sensitivity measurement, and peak fitting, as discussed in the text.

3.2. Underlying peak of zirconium

A consistent discrepancy is observed between CNPGAA results and those given by VHE which is necessary to rationalize. The first hypothesis considered was that not all the hydrogen was extracted during VHE so that some hydrogen remained in the sample, leading to a lower value in VHE measurement. To test this hypothesis, we used IGF on the same samples, which should release all the hydrogen. We obtained the same results as in VHE, which confirmed that no hydrogen remained in the samples after VHE.

The second hypothesis considered is that there is an underlying peak at the hydrogen gamma ray energy (since the discrepancy is constant among the different zirconium alloys investigated, it should be a zirconium peak). However no zirconium peak is referenced at this energy [22] and no effects such as a double-escape peak, pair-production or Bremsstrahlung escape peaks could explain it. It is likely that this particular peak of zirconium has never been previously reported because all zirconium samples contain a small amount of hydrogen and researchers may have ascribed that peak to the hydrogen [23]. Indeed, hydrogen is very stable in zirconium and is normally present in zirconium after the processing of the material [24]. According to VHE results on bare alloys in Table 2, the initial hydrogen concentration after processing is usually on the order of 10 wt.ppm. The previous studies using CNPGAA on zirconium alloys to detect other elements than hydrogen would not have examined this particular peak which was supposed to be only due to hydrogen. To check if there was an unknown underlying peak of zirconium we first performed VHE on four different zirconium alloys to obtain hydrogen-free zirconium samples, which were then examined using CNPGAA. The hydrogen-free zirconium samples also showed a constant peak at the hydrogen energy, which supports the hypothesis of the unknown underlying zirconium peak. Note that to perform VHE on the samples, it has been necessary to cut them using a low speed diamond saw to a size of 4 mm x 8 mm x 0.8 mm. Likely because of this or because of some remaining traces of hydrogen in the degassed samples, the value of the observed peak in free hydrogen samples was slightly higher than in the full sized hydrided samples used in Table 2.

To conclude, for samples in which the neutron beam area is entirely covered by the sample or larger, the underlying zirconium peak is equal to 29.4 ± 1.1 wt.ppm of hydrogen. Taking into account this underlying peak of zirconium and as long as the sample area fully covers the

neutron beam, CNPGAA technique accurately matches the results given by conventional destructive techniques such as VHE.

3.3. Hydrogen concentration as function of corrosion time using CNPGAA

Since the above measurements show that CNPGAA technique is reliable to determine hydrogen concentration in zirconium alloys once the underlying peak of zirconium is taken into account, we used the technique to measure hydrogen content on two individual ZIRLO coupons (2.5 mm x 3.0 mm x 0.8 mm) at different times during the corrosion process. The ZIRLO coupons were corroded under the same conditions as the alloys shown in Table 2: 360 °C pure water in a single static autoclave of 4 liters in saturated pressure condition at 2708.6 psi (18.7 MPa). Several ZIRLO sister samples were inserted in the autoclave to study the evolution of hydrogen uptake using VHE. The results are presented in Figure 4 which plots the weight gain (mg.dm^{-2}, on the right scale) caused by the uptake of oxygen during the corrosion reaction for every samples analyzed by VHE or CNPGAA at that particular corrosion time. The hydrogen contents (on the left vertical axis) were measured using both CNPGAA and VHE. The results shown in Figure 4 indicate that taking out one ZIRLO coupon, performing CNPGAA on it and then inserting it back to the autoclave does not appear to alter the corrosion process. For instance, after 75 days of corrosion, one of the sister samples used in VHE (cross) and coupon two (circle) contain, at that particular corrosion time, the same amount of hydrogen, even though coupon two underwent two CNPGAA measurements (one at 35 days and on at 75 days). The examination of the evolution of hydrogen content among the different samples allow us to conclude that CNPGAA coupons behave similarly to sister samples, and thus the CNPGAA measurement does not alter the corrosion process and hydriding of ZIRLO samples. One should note that the error bars of CNPGAA are consistently smaller than those of VHE throughout the corrosion process, which

confirms that CNPGAA is more precise than VHE. The hydrogen concentrations and weight gains measured can be used to calculate the hydrogen pick-up fraction as a function of corrosion time. This has been done using the values from Figure 4 and hydrogen pick-up fraction is plotted in Figure 5. This means that the technique can be used for measuring hydrogen uptake during corrosion of zirconium alloys, which will be the subject of upcoming publications.

At the beginning of the corrosion process, corrosion rate is high and the pick-up fraction increases rapidly to reach a value of approximately 10%. The hydrogen pick-up fraction remains more or less equal to 10% in this pre-transition regime following a decrease in the corrosion rate (see weight gain curve in the right scale). Then, after approximately 70 days of corrosion, it starts to increase again up to approximately 23%. This increase occurs before the corrosion weight gain transition, which occurs around 95 days of corrosion. Thus, the hydrogen pick-up fraction increases before the sudden loss of protectiveness occurring at the weight gain transition, which indicates that, even if the corrosion rate is still low, more hydrogen is picked-up by the sample. After the weight gain transition, the hydrogen pick-up fraction remains constant but at a higher value compared to before the transition. This general behavior has already been reported by Harada et al. [7]. However, no satisfactory mechanism has been found to explain it. Additional experiments are done at this moment to understand the mechanism leading to this hydrogen pick-up fraction behavior.

Conclusion

The Cold Neutron Prompt Gamma Activation Analysis method was applied to non-destructive hydrogen level assessment in Zr alloys. CNPGAA has been shown to be a reliable, accurate and precise method to determine hydrogen concentration in zirconium alloys, if one is careful to take into account the non-referenced underlying peak of zirconium at the hydrogen gamma ray energy

16

of 2223 keV in calculating the hydrogen concentration and ensuring that the sample completely covers the beam. The CNPGAA technique is non-destructive, does not affect the corrosion process and measures the hydrogen concentration of the whole coupon, thus avoiding any spot-to-spot variation of hydrogen concentration (which can become significant close to the oxide transition). Also, CNPGAA can precisely detect low levels of hydrogen (as low as 5 wt.ppm) and can be used to measure the variations of hydrogen concentration in a single sample which makes it more attractive than other non-destructive techniques developed. Hydrogen pick-up fraction of ZIRLO samples has also been investigated using CNPGAA and VHE. It is shown that the hydrogen pick-up fraction undergoes significant increases at the beginning of the corrosion and slightly before the weight gain transition. The increase of hydrogen pick-up fraction before the weight gain transition is not well understood and is currently under investigation.

Acknowledgements

References

[1] Corrosion of Zirconium Alloys in Nuclear Power Plants, IAEA-TECDOC-684, Vienna, 1993.

[2] Waterside corrosion of zirconium alloys in nuclear power plants, IAEA-TECDOC-996 Vienna, 1998.

[3] S. Kass, Journal of The Electrochemical Society, 107 (1960) 594-597.

[4] H.H. Klepfer, Corrosion, 19 (1963) 285.

[5] W.E Berry, D.A. Vaughan, E.L. White, Corrosion, 17 (1961) 109.

[6] B. Cox, Journal of Nuclear Materials, 264 (1999) 283-294.

[7] M. Harada, R. Wakamatsu,in: Zirconium in the Nuclear Industry: 15th International Symposium, ASTM, 2008, pp. 384.

[8] E.A. Gulbransen, Andrew, K. F., Journal of The Electrochemical Society, 116 (1969) 659-664.

[9] M. Nakatsuka, S. Ishimoto, Y. Ishii, A. Miyazaki, Journal of Nuclear Science and Technology, 43 (2006) 1142-1148.

[10] M.P. Gómez, G. Domizzi, M.I.L. Pumarega, J.E. Ruzzante, Journal of Nuclear Materials, 353 (2006) 167-176.

[11] L. Bennun, J. Santisteban, J. Díaz-Valdés, J.R. Granada, R.E. Mayer, Nuclear Instruments and Methods in Physics Research Section B: Beam Interactions with Materials and Atoms, 263 (2007) 468-472.

[12] Methods of Chemical Analysis of Zirconium and Zirconium Alloys (Silicon, Hydrogen, and Copper), ASTM E146-83

[13] Standard Test Method for Determination of Hydrogen in Titanium and Titanium Alloys by the Inert Gas Fusion Thermal Conductivity/Infrared Detection Method, ASTM E1447 - 09

[14] W.P. Reed,Certificate of Analysis Standard Reference Material 352c, National Institute of Standards and Technology, 1990.

[15] R. Paul, Analyst, 122 (1997) 35R-41R.

[16] R. Paul, R. Lindstrom, A. Heald, Journal of Radioanalytical and Nuclear Chemistry, 215 (1997) 63-68.

[17] R. Paul, R. Lindstrom, C. Brocker, E. Mackey, Journal of Radioanalytical and Nuclear Chemistry, 278 (2008) 697-701.

[18] R. Lindstrom, Biological Trace Element Research, 43-45 (1994) 597-603.

[19] A.T. Motta, M.J. Gomes Da Silva, A. Yilmazbayhan, R.J. Comstock, Z. Cai, B. Lai,in: Zirconium in the Nuclear Industry: 15th International Symposium, ASTM, 2009, pp. 486.

[20] E.A. Mackey, R.L. Paul, R.M. Lindstrom, D.L. Anderson, Journal of Radioanalytical and Nuclear Chemistry, 265 (2005) 273-281.

[21] D. Gaskill,Vice President General Manager LUVAK. Inc,in, Personal Communication, 2010.

[22] Database of Prompt Gamma Rays from Slow Neutron Capture for Elemental Analysis, IAEA STI/PUB/1263, 2007.

[23] S. Nakamura, H. Harada, S. Raman, P.E. Koehler, Journal of Nuclear Science and Technology, 44 (2007) 21-28.

[24] E.A. Gulbransen, K.F. Andrew, Journal of The Electrochemical Society, 101 (1954) 474-480.
[25] R. Paul, E. Mackey, Journal of Radioanalytical and Nuclear Chemistry, 181 (1994) 321-333.

Figure Captions

Figure 1: Plan of the NIST reactor and the Cold Neutron Research Facility. The guide hall dimensions are 30.5x61m.

Figure 2: Gamma ray counts versus gamma ray energy obtained during measurement of a Zr-1Nb-1Sn-0.1Fe sample after 105 days of corrosion in pure water at 360°C and plotted using a commercial peak search program. In gray and indicated by arrows, are the zirconium reference peak (934keV) and the hydrogen peak (2223keV).

Figure 3: Zoom of the gamma ray spectrum (number of counts in function of gamma ray energy) on the hydrogen energy peak region of Zr-1Nb-1Sn-0.1Fe after 105 days of corrosion in pure water at 360°C, plotted using a commercial peak search program. The hydrogen peak is indicated by an arrow. The calculated hydrogen concentration of this alloy after 105 days of corrosion is 49wt.ppm.

Figure 4: Hydrogen concentration (wt.ppm) in ZIRLO coupons as function of corrosion time using VHE on sister samples and successive CNPGAA measurements on two different individual coupons, plotted along with the weight gain of the corresponding sample. Error bars represent 1s uncertainties based on counting statistics, sensitivities , and peak fitting, as discussed in the text.
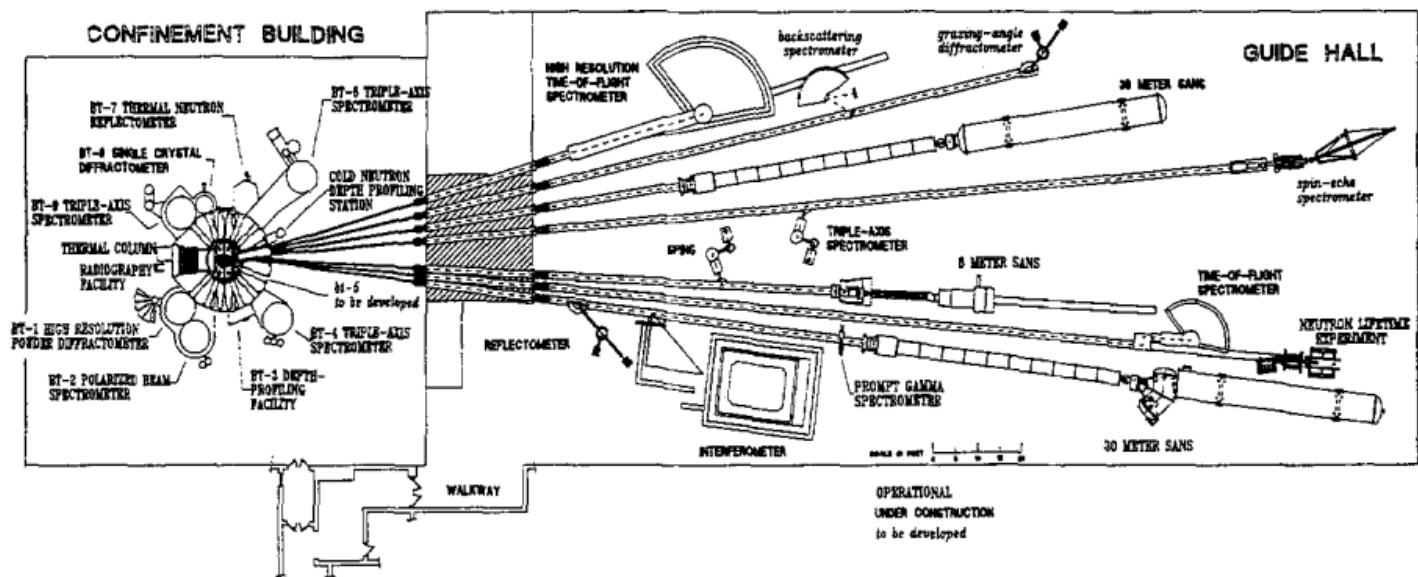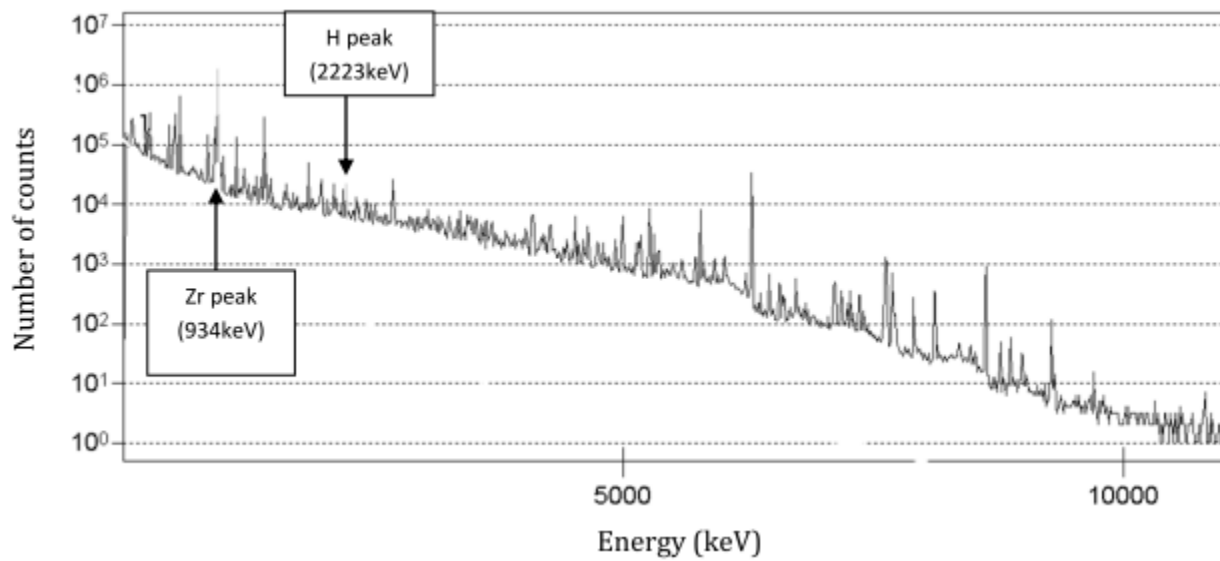
Figure 5: Hydrogen pick-up fraction in ZIRLO coupons as function of corrosion time, plotted along with the weight gain of the corresponding coupon. Error bars represent 1s uncertainties based on counting statistics, sensitivities , and peak fitting, as discussed in the text.
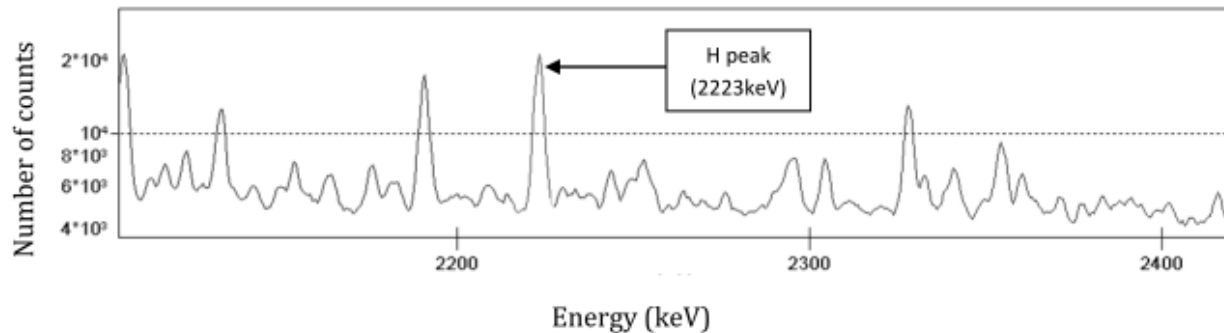
Figure 1:

Figure 2:
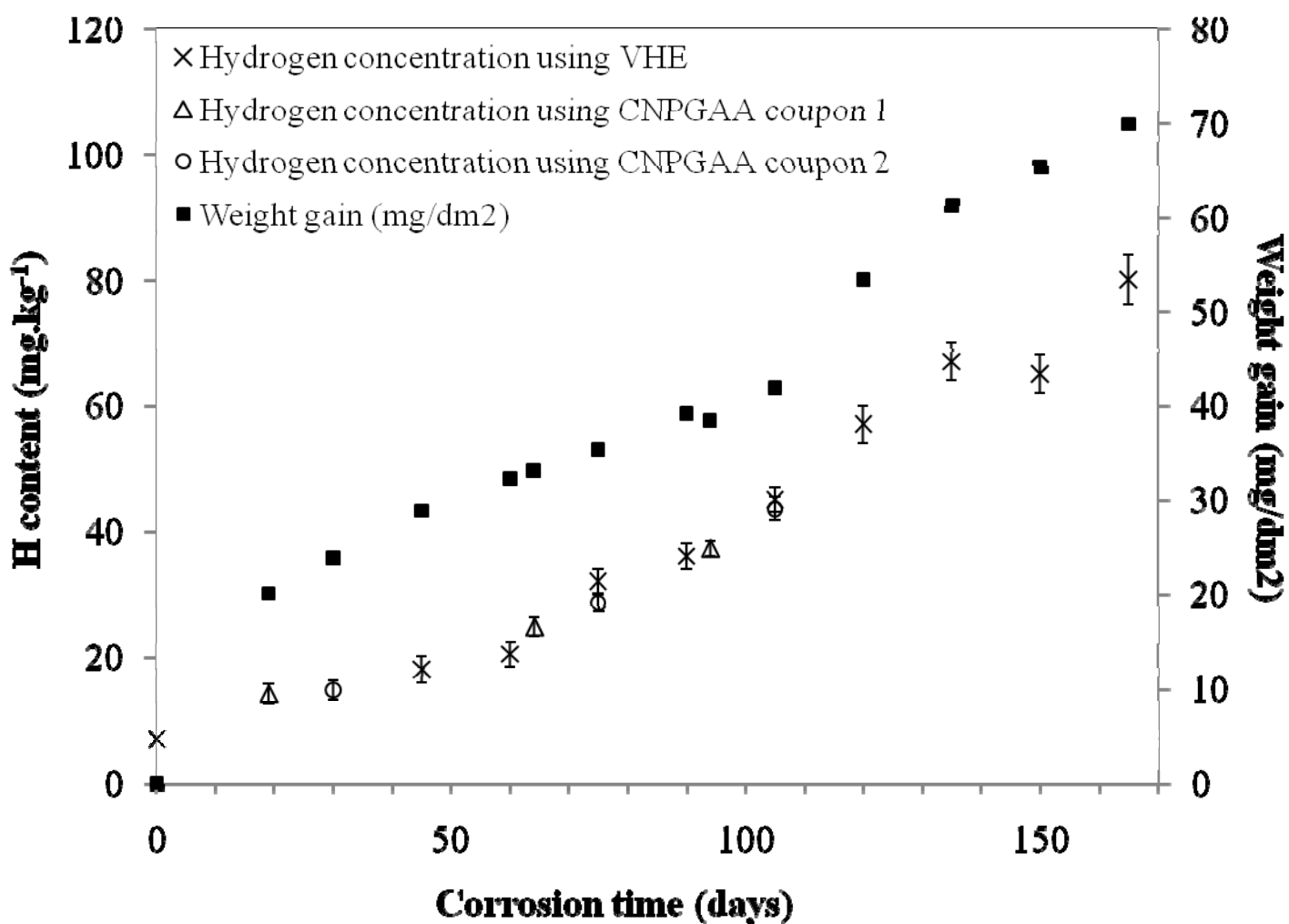
Figure 3:

Figure 4:

Figure 5: